MR of Osteochondritis Dissecans and Avascular Necrosis of the Mandibular Condyle

Kurt P. Schellhas, Clyde H. Wilkes, Hollis M. Fritts, Mark R. Omlie and Lawrence B. Lagrotteria

AJNR Am J Neuroradiol 1989, 10 (1) 3-12
http://www.ajnr.org/content/10/1/3

MR of Osteochondritis Dissecans and Avascular Necrosis of the Mandibular Condyle

Kurt P. Schellhas[1]
Clyde H. Wilkes[2]
Hollis M. Fritts[1]
Mark R. Omlie[3]
Lawrence B. Lagrotteria[4]

We studied 40 patients exhibiting radiologic changes of either osteochondritis dissecans (OCD) or avascular necrosis (AVN) involving the mandibular condyle to evaluate the structural changes associated with these lesions when using high-field-strength MR imaging. Various clinical indications for imaging each patient with routine radiography, tomography, and surface-coil MR included headache, temporomandibular joint (TMJ) and/or ilsilateral facial pain, joint crepitus, clicking, locking, and either recently acquired or changing (unstable) occlusal disorder. Radiologic findings included alterations in condyle morphology and MR signal characteristics compatible with either OCD or AVN or, in some cases, both. Previous nonsurgical mandibular trauma was temporally related to the onset of symptoms in eight patients. Five patients exhibiting either unilateral or bilateral AVN involving the condyles and condylar necks had undergone previous orthognathic surgery, including sagittal split mandibular osteotomies followed by intermaxillary fixation. One patient exhibiting condylar AVN with articular surface collapse and osseous destruction had undergone previous TMJ meniscectomy followed by insertion of a permanent Proplast implant. Thirty-one of 34 patients with no prior surgery and MR changes of condylar OCD/AVN had associated internal derangement of the TMJ meniscus. There was surgical confirmation of findings in 10 joints.

We assert that OCD and AVN are relatively common, clinically significant lesions of the mandibular condyle often associated with preexisting internal derangement of the temporomandibular joint.

Avascular (aseptic) necrosis (AVN) of the mandibular condyle is a relatively common disorder that is generally not recognized [1–5]. MR imaging is established as a highly sensitive and accurate procedure for the diagnosis of early osteochondritis dissecans (OCD) and AVN [6–17]. MR also has emerged as the procedure of choice for demonstration of internal derangements of the temporomandibular joint (TMJ) [3–5, 18–21]. Lesions with radiologic features of OCD and AVN involving the mandibular condyle and condylar neck are demonstrable with MR. Our intention is to demonstrate the appearance of these clinically significant but frequently unrecognized disorders with the use of high-field MR.

Materials and Methods

Forty patients (35 females and five males 14–61 years old, 45 joints) with MR findings compatible with either OCD or AVN were selected for study. All patients were evaluated with radiography, including submentovertex and anteroposterior, open-mouth, jaw-protruded radiographs; tightly collimated closed- and open-mouth lateral TMJ tomograms; and surface-coil MR. Indications for imaging included headache, TMJ and/or ipsilateral facial pain, joint crepitus, clicking and/or locking, and either acquired or changing malocclusion within 12 months of clinical evaluation (Table 1). Radiographic-tomographic findings considered suggestive of either AVN or OCD included alterations in condyle morphology, such as sharply defined articular surface defects (OCD) and either focal or generalized articular surface collapse (AVN). Associated findings such as hypertrophic spurs and articular sclerosis in either the temporal bone or condyle were noted. Selected patients with severe deformity on radiographs

This article appears in the January/February 1989 issue of *AJNR* and the March 1989 issue of *AJR*.

Received February 26, 1988; accepted after revision June 31, 1988.

Presented at the annual meeting of the American Society of Temporomandibular Joint Surgeons, Miami, FL, February 1988, and in part at the annual meeting of the American Association of Oral and Maxillofacial Surgeons, Boston, October 1988.

[1] Center for Diagnostic Imaging, 5775 Wayzata Blvd., Suite 190, St. Louis Park, MN 55455. Address reprint requests to K. P. Schellhas.

[2] Park Place Center, 5775 Wayzata Blvd., Suite 990, St. Louis Park, MN 55416.

[3] 250 Central Ave. N., Wayzata, MN 55391.

[4] 801 N. Plaza Dr., Suite 106, Schaumberg, MN 55455.

***AJNR* 10:3–12, January/February 1989**
0195–6108/89/1001–0003

TABLE 1: Clinical Symptoms Associated with Osteochondritis Dissecans and/or Avascular Necrosis Involving the Mandibular Condyle

Symptom	No. of Joints (n = 45)	No. of Patients (n = 40)
Headache/facial pain	–	36
TMJ pain	37	33
Malocclusion (acquired or changing in recent 12 months)	–	24
TMJ clicking or locking	35	33
TMJ crepitus	17	15

Note.—TMJ = temporomandibular joint.

and tomograms were studied with unenhanced, consecutive 1.5-mm-thick axial CT images that were input to a three-dimensional processor for generation of discrete voxel faces and three-dimensional images for two-dimensional viewing [22].

Most MR studies were performed with a single, commercially available, 8.9-cm, round, receive-only surface coil. Patients were scanned supine, with their heads rotated 10–15° toward the coil (cephalometric correction) and resting within the surface coil holder. The patients' heads were secured to the coil with tape. A short, 10-mm-thick partial-flip-angle or GRASS (gradient-recalled acquisition in the steady state) axial localizing sequence, 21/9 (TR/TE), was used with a flip angle of 30°, 24-cm field of view (FOV), 128 × 256 matrix, and three images requiring 9 sec. Seven or eight 3-mm-thick (1-mm gap) closed-mouth sagittal images were obtained thereafter through the full width of the mandibular condyle, 600–2500/20,80–100/2 (TR range/first-echo TE, range of second-echo TEs/excitations), 12-cm FOV, 256 × 256 matrix. Most routine studies of the TMJ were evaluated with T1-weighted images, 600/20, while cases of suspected AVN or OCD were studied with multiecho pulse sequences, 2000–2500/20,80–100/1, 3-mm thick, 1-mm gap, and 256 × 256 matrix. Most patients with morphologic and/or signal changes suggestive of OCD or AVN on T1-weighted images were subsequently studied with multiecho, T2-weighted images. Further details of single-coil technical parameters have been described previously [3, 4].

After equipment and software upgrading, recent studies were performed with a dual 8.9-cm round, bilateral, receive-only surface-coil setup, with coupled coils to prevent RF feedback. Patients were scanned supine with their heads in the neutral position (not tilted). Surface coils were positioned over the TMJs and secured tightly to the patient's head (without tape) to reduce motion. A preliminary axial sequence, 300/20/1, with three 5-mm-thick images was obtained for the purpose of condylar localization. Seven to nine nonorthogonal 3-mm images, 700–2500/20,80–100, with a 1-mm gap were obtained thereafter through the full width of each condyle, scanning perpendicular to the long condylar axis (Fig. 1). A typical T1-weighted sequence, 700/25/2, required 12 min. Owing to gradient restrictions, a minimum TR of 700 msec was required to simultaneously obtain images through the full width of each condyle, and a TE of 25 msec was required to obtain a 12-cm FOV. These same gradient restrictions also required the use of both slightly longer first-echo TEs on the multiecho sequences and slightly longer TRs on the bilateral GRASS studies to achieve a small, high-resolution FOV. After initial experimentation, a routine multiecho sequence, 2200/25,80/1, with a 13-cm FOV was established that required 9 min 51 sec. GRASS images were obtained routinely through each joint simultaneously, scanning perpendicular to the condylar axis by using a single 5-mm-thick, midcondylar nonorthogonal slice, 30/13/2, with a 30° flip angle and 16-cm FOV. GRASS images were obtained in closed, half open, and fully open mouth positions in each patient. Total scanning time for a routine, bilateral examination with either 700/20/2 or multiecho 2200/20,80/1 images averaged about 30 min. Coronal, unilateral 3-mm-thick, 12-cm FOV images, 700–800/20/2, were obtained in selected cases when alterations of condylar morphology and/or marrow signal characteristics were observed on either sagittal MR images or preliminary radiographs and tomograms.

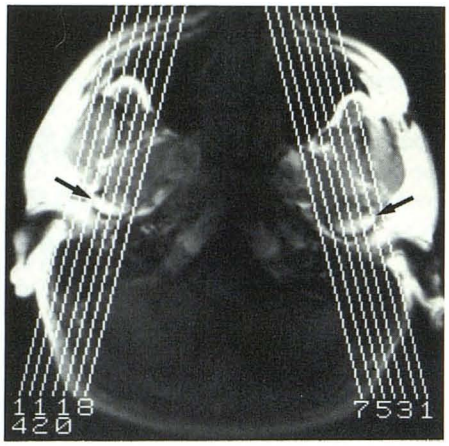

Fig. 1.—Axial 5-mm localizing image, 300/20, shows mandibular condyles (*arrows*) and sagittal image orientation (*lines*) during bilateral study with dual surface coils.

Results

Clinical abnormalities in the 40 patients studied included headache and/or either unilateral or bilateral facial pain (36 patients), localized TMJ pain, recently acquired or changing malocclusion within 12 months of clinical evaluation, and TMJ clicking or locking and joint crepitus (Table 1). Patients frequently described the occlusal alterations as fluctuating in direct relation to the severity of joint pain, interpreted to reflect variation in degrees of joint inflammation. A clear history of previous nonsurgical mandibular trauma was temporally related to the onset of malocclusion and joint symptoms in eight patients. Five patients exhibiting either unilateral or bilateral AVN involving the proximal mandibular segments (condyles and condylar necks) had undergone orthognathic surgery (without preoperative TMJ imaging beyond cephalometric radiographs) within 24 months of evaluation, including bilateral sagittal split mandibular osteotomies, followed by rigid intermaxillary fixation. Joint effusion was observed in 30 patients and in all 18 patients (and joints) studied with T2-weighted images. One patient with a 3-week history of TMJ pain and MR findings including intraarticular fluid (inflammatory arthropathy), meniscus displacement and deformity, and subacute AVN had undergone 6 weeks of nonsurgical, pull-forward mandibular repositioning for occlusal adjustment with external head gear immediately before imaging. One patient with bilateral condylar AVN had previous AVN of the femoral head. One patient had undergone previous TMJ meniscectomy followed by insertion of a permanent implant made of Proplast.* Thirty-one of 34 patients with no previous surgery

* Vitek, Houston, TX.

(neither TMJ nor orthognathic) and MR findings of condylar OCD/AVN had associated internal derangement of the TMJ meniscus.

Radiographic and tomographic studies were abnormal and suggestive of either OCD or AVN in 32 of the 40 patients studied. Radiographic and tomographic abnormalities observed included side-to-side asymmetry in mandibular condyle morphology, discrepancies in condyle and condylar neck height, focal or generalized articular surface depressions, articular surface and/or condylar sclerosis, focal articular surface defects (suggesting OCD), widening or narrowing of the articular space on closed-mouth lateral tomograms, gross decrease in condyle size, and deviation of the chin toward a shortened and/or deformed condyle or proximal mandibular segment.

MR findings observed in the series included alterations in condylar morphology (paralleling tomographic observations) and decreased condylar marrow signal on short or long TR/short TE sequences and either decreased, variable, or increased marrow signal on GRASS and T2-weighted images. Signal changes within the condylar marrow were observed with or without accompanying morphologic alterations (Tables 2 and 3). Focal, sharply defined articular surface defects, where cortical bone appeared to be either missing or of low signal intensity and depressed, were interpreted to represent OCD (Figs. 2–4) [15]. Focal, subarticular, and/or generalized condylar lesions with decreased first-echo marrow signal, 600–2500/20–25, and either decreased, variable, or increased T2 (and/or GRASS) signal, with or without morphologic alterations, were considered suspicious for AVN (Figs. 3–15). Four patients (five joints) had distinct MR findings of both OCD and AVN in the same condyle (Figs. 14 and 15).

Ten patients (10 joints) from the series have had surgery for either meniscectomy (nine patients) or joint debridement, permanent implant removal, and attempted reconstructive arthroplasty (one patient). Focal articular cartilaginous defects were seen overlying areas of cortical depression and/or collapse, with either stable or dislocated (unstable) osseous fragments (Figs. 2, 3, 9, 14, and 15). Organizing clots were found within articular surface defects where bone had either collapsed or a fragment had become dislodged (Figs. 2, 9, 14, and 16). Erosion of articular-bearing-surface cartilage and localized cortical irregularity was a common finding in condyles where suspected OCD/AVN was associated with late-stage internal derangement of the TMJ. Extensive capsular fibrosis and old hemarthrosis were encountered within the adherent joint capsules of three joints in conjunction with condylar changes of OCD and AVN (Fig. 14). Localized periosteal and medullary hyperemia was found in two cases with MR findings suggesting acute or subacute AVN. Severe bone softening, articular surface collapse, osseous destruction, and granulomatous inflammation were encountered during removal of the permanent Proplast TMJ implant (Fig. 17) [3, 5].

TABLE 2: Summary of Radiologic Diagnoses in Patients with MR Findings of Osteochondritis Dissecans or Avascular Necrosis of the Mandibular Condyle

Diagnosis	No. of Patients
Localized or subarticular avascular necrosis	23
Avascular necrosis of entire condyle	7
Osteochondritis dissecans	10
Total	40
Osteochondritis dissecans and/or avascular necrosis with meniscus derangement (no previous surgery)	31/34
Osteochondritis dissecans and avascular necrosis	4

Discussion

OCD and AVN are pathologic entities with definite similarities. Both lesions involve the articular surfaces of joints and may represent a spectrum of the same pathophysiology, necrosis of bone [1, 3–17, 23–27]. OCD is often a consequence of transchondral fracture, where the depressed cortical bone fails to heal or reunite to adjacent normal bone and may become mobile or unstable, depending on the integrity of overlying articular cartilage (Figs. 2–4) [27]. OCD is usually a localized process and is most often observed in the medial femoral condyle and less commonly in remaining appendicular joints. AVN generally describes a large area of cortical and medullary infarction, often resulting in structural weakening, which predisposes the joint to collapse and osseous degeneration (Figs. 5–17) [6–17, 23–27]. Both entities may be associated with underlying hematologic disorders, skeletal dysplasias, chemotherapeutic agents, including exogenous

TABLE 3: MR Signal Characteristics of Normal and Pathologic Mandibular Condyles

Condition	Sequence/Signal Characteristics			
	T1	Intermediate	T2	GRASS
Normal condyle	Increased	Increased or variable	Variable or decreased	Decreased
Early (acute) avascular necrosis	Decreased	Decreased or variable	Increased	Variable or increased
Late avascular necrosis	Decreased	Decreased	Decreased	Decreased
Osteochondritis dissecans	Decreased	Decreased or variable	Decreased to increased[a]	Increased to decreased[a]
Healing	Decreased	Variable	Increased or variable	Increased or variable

Note.—GRASS = gradient-recalled acquisition in the steady state.

[a] Highly variable.

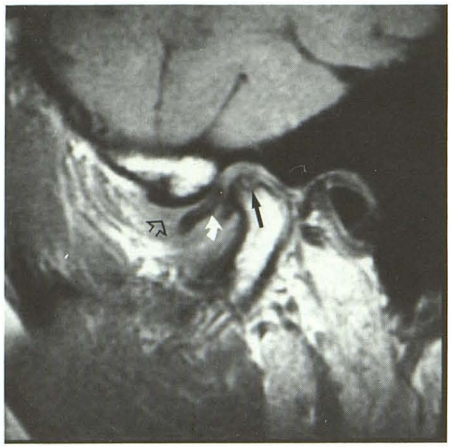

Fig. 2.—Histologically confirmed osteochondritis dissecans (*solid straight arrow*) and inflammatory temporomandibular joint arthropathy in 42-year-old woman after 10 weeks of severe joint pain, locking, and crepitus. The patient had osteochondritis dissecans in the knee 12 months before. Sagittal image, 600/20, also shows fluid (*open arrow*) above anteriorly displaced meniscus (*curved arrow*). Symptoms were completely relieved by meniscectomy and joint debridement of adhesions.

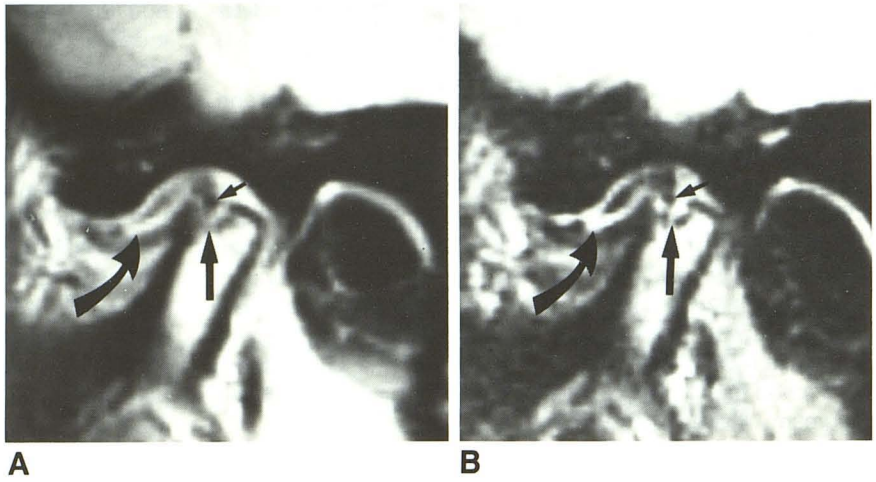

Fig. 3.—Osteochondritis dissecans (*long straight arrows*) causing pain and occlusal change in 34-year-old woman. Sagittal images, 2200/25 (*A*) and 2200/80 (*B*), show intraarticular effusion (*curved arrows*) with focal articular fragment (*short straight arrows*) surrounded by zone of high signal.

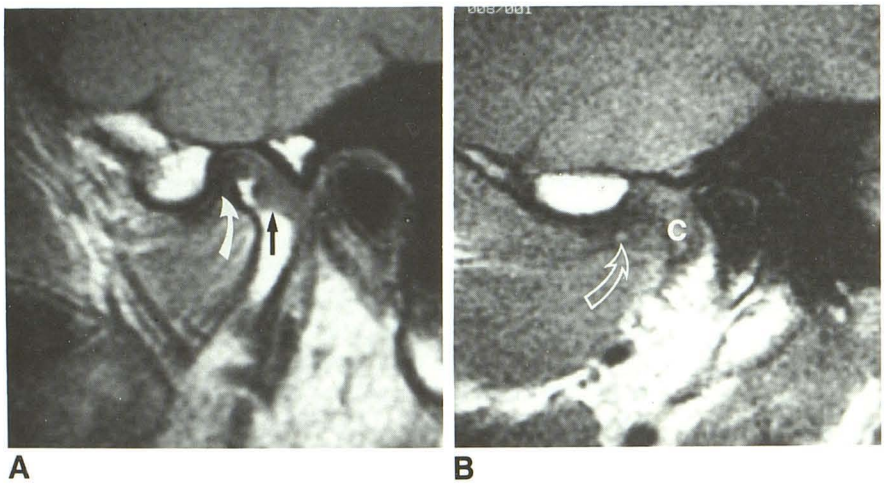

Fig. 4.—Osteochondritis dissecans with free condylar fragment in 36-year-old man with temporomandibular joint pain for 4 months before imaging and intermittent pain, crepitus, and locking at time of imaging.

A, Sagittal closed-mouth image, 600/20, through mid condyle reveals sharply defined posterior condylar defect (*black arrow*) and normal meniscus (*curved arrow*).

B, Image through medial pole of condyle (c) reveals viable condylar fragment (*arrow*) with mildly diminished signal. Joint exploration advised; patient refused surgery.

steroid administration, trauma, decompression (barotrauma), and familial predisposition [12, 14, 24, 25].

The clinical features of OCD/AVN are characterized by pain and joint disability, often leading to skeletal deformity [12, 14, 24, 25, 27]. Facial pain localized to the mandibular division of the trigeminal nerve (V_3), including the muscles of mastication and TMJ, is a common feature of acute and subacute OCD and/or AVN involving the proximal mandible (Table 1). The pain may be described as either constant in duration or pulsatile and exacerbated by joint movement, particularly if there is coexistent joint inflammation and internal derangement of the adjacent TMJ meniscus (Figs. 2–10, 14, and 16). Ipsilateral headache, earache, and masticatory muscle pain and spasm are observed with or without mechanical joint symptoms, suggesting pain referral throughout the trigeminal nerve distribution. Limitation of joint movement is commonly observed. Joint crepitus is common and may reflect degenerative osseous changes, loose bodies, adhesions, or the presence of joint effusion (Figs. 2–6, 8–10, and 12–17) [4]. Occlusal changes are common findings with all stages of OCD and AVN. Fluctuating or unstable malocclusion is observed frequently with joint effusions and appears to vary with the amount of fluid within the joint (Figs. 2, 3, 7, 9, 10, 14, and 17). Subchondral fracture, collapse, and remodeling of the condyle appear to occur in the mandible with pathologic events similar to those described for other joints (Figs. 5, 6,

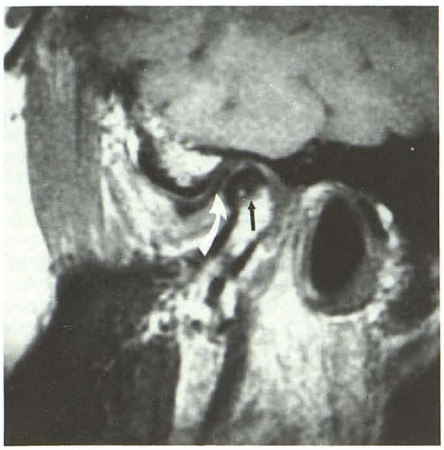

Fig. 5.—Subarticular avascular necrosis of mandibular condyle associated with internal derangement of temporomandibular joint meniscus in 34-year-old woman with 1 year history of temporomandibular joint clicking and crepitus and 3-month history of constant joint pain and acquired, fluctuating crossbite. MR image, 600/20, shows subarticular marrow hypointensity (*straight arrow*) beneath anteriorly displaced meniscus (*curved arrow*).

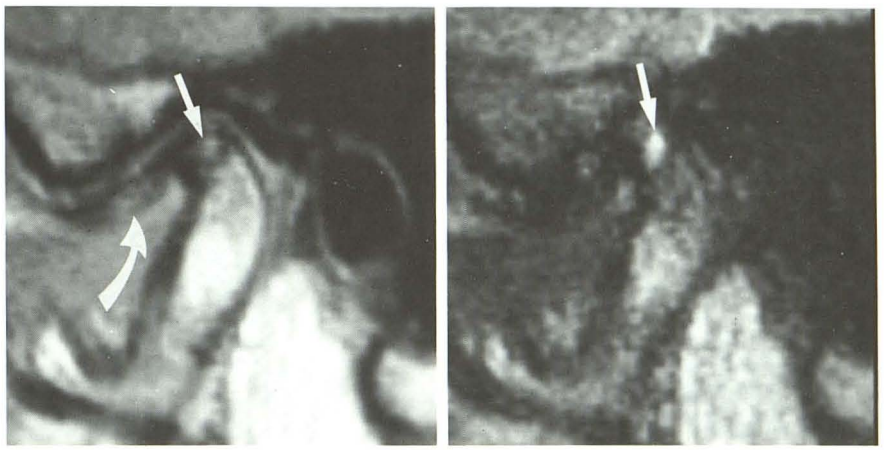

A B

Fig. 6.—Subacute avascular necrosis with advanced internal derangement of temporomandibular joint in 61-year-old man with long history of temporomandibular joint clicking and recent onset of joint pain. Sagittal images, 2200/25 (*A*) and 2200/80 (*B*), show displaced and thickened meniscus (*curved arrow*) exhibiting high signal due to myxomatous degeneration. Subarticular condyle defect (*straight arrows*) exhibits intermediate (*A*) and high (*B*) signal.

Fig. 7.—Subacute avascular necrosis with advanced internal derangement of temporomandibular joint associated with forward mandibular protrusion caused by intraoral splint and external head gear for attempted disk repositioning (no prior imaging procedures). This 14-year-old girl had malocclusion, 6-month history of temporomandibular joint locking, and 3-week history of intense joint pain after application of appliances.

A, Sagittal closed-mouth image, 600/20, shows condylar deformity with hypointense marrow signal (*arrow*). Meniscus (*arrowhead*) anteriorly displaced. Note widened joint space with absence of defined posterior meniscus attachment.

B, Sagittal image, 2200/100, reveals increased marrow signal (*straight arrow*) owing to medullary fluid. Superior compartment effusion (*curved arrow*) is present above swollen posterior attachment (above condyle). *Arrowhead* denotes displaced meniscus. Joint pain and tenderness promptly abated after removal of appliances.

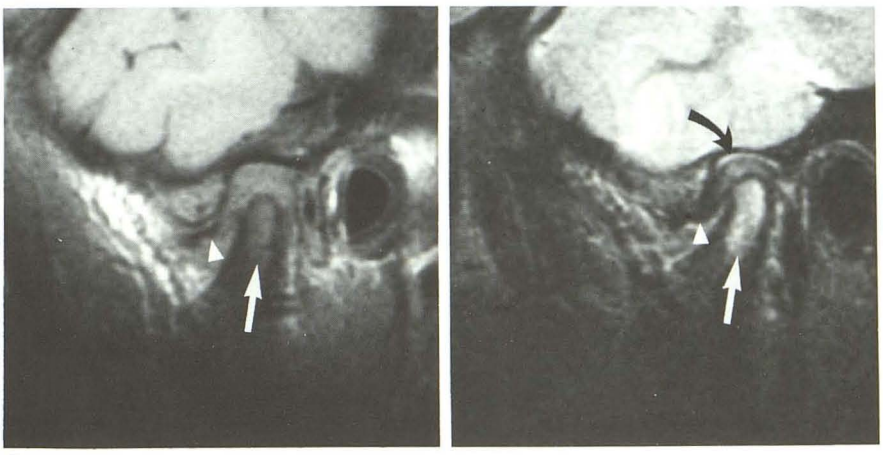

A B

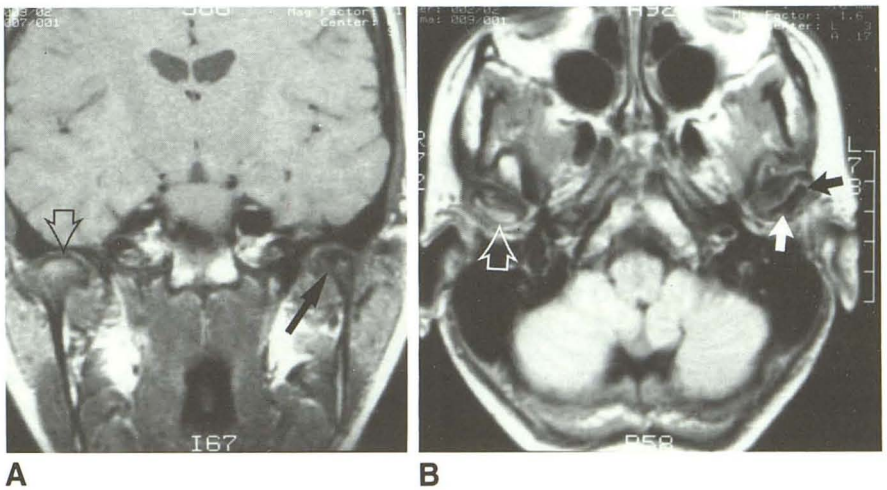

A B

Fig. 8.—Old condylar avascular necrosis and deformity in 39-year-old woman with 3-month history of left-sided facial pain, temporomandibular joint locking, and malocclusion. (Study performed with head coil to evaluate "headache.")

A, Coronal image, 800/20, reveals hypointense and deformed left condyle (*solid arrow*) compared with normal right side (*open arrow*).

B, Axial image, 2000/20, shows condylar deformity and loss of marrow signal (*solid arrows*) compared with normal side (*open arrow*). Patient refused further investigation.

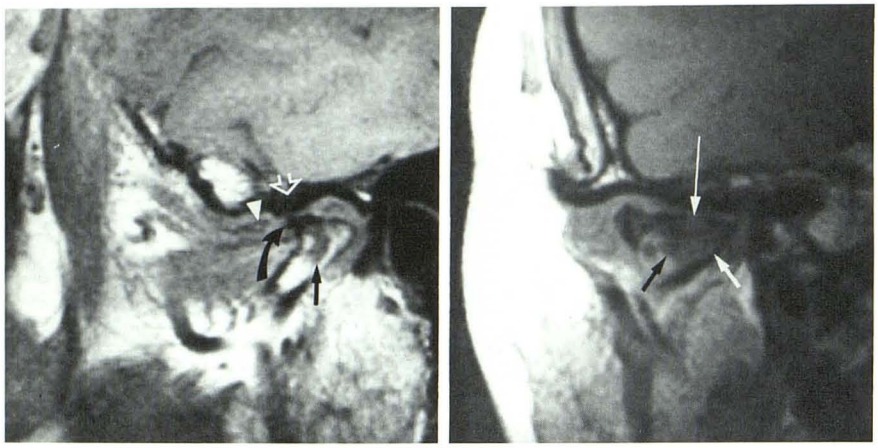

Fig. 9.—Osteoarthritis with suspected old avascular necrosis in 55-year-old woman with 5-year history of progressive crossbite, crepitus, and severe joint pain and locking (opposite side clinically and radiologically normal).

A, Sagittal closed-mouth image, 600/20, reveals deformed condyle with area of diminished marrow signal (*straight solid arrow*). Condylar osteophyte (*curved arrow*) lies beneath remodeled and sclerotic articular eminence (*open arrow*) of temporal bone. Degenerated meniscus (*arrowhead*) anterior to large perforation.

B, Coronal image shows flattened and deformed condyle with large area of diminished signal (*short arrows*) beneath articular surface defect (*long arrow*). Organized scar within articular surface depression was found at surgery.

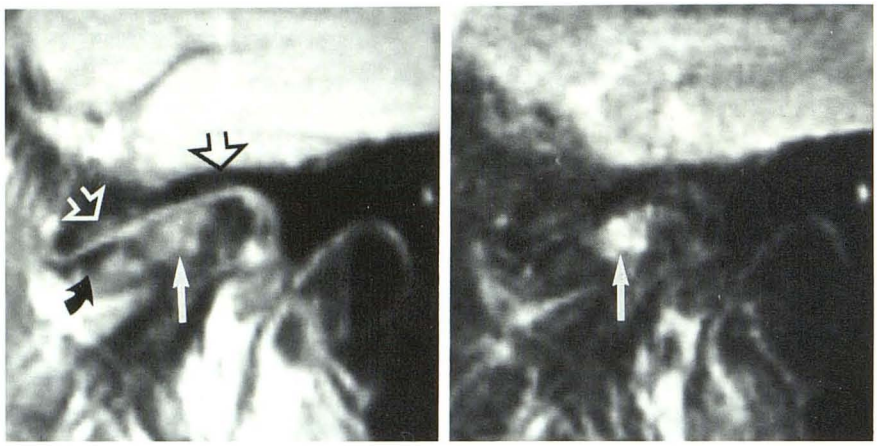

Fig. 10.—Early avascular necrosis with old, advanced temporomandibular joint derangement and bony remodeling in 59-year-old woman with unstable occlusion and joint pain, crepitus, and locking. Sagittal images, 2200/25 (*A*) and 2200/80 (*B*), show degenerated meniscus (*curved arrow*) in front of deformed condyle. Large area of subarticular avascular necrosis (*straight solid arrows*) beneath flattened and thickened temporal bone surface (*open arrows*). Joint fluid was seen on adjacent images (not shown).

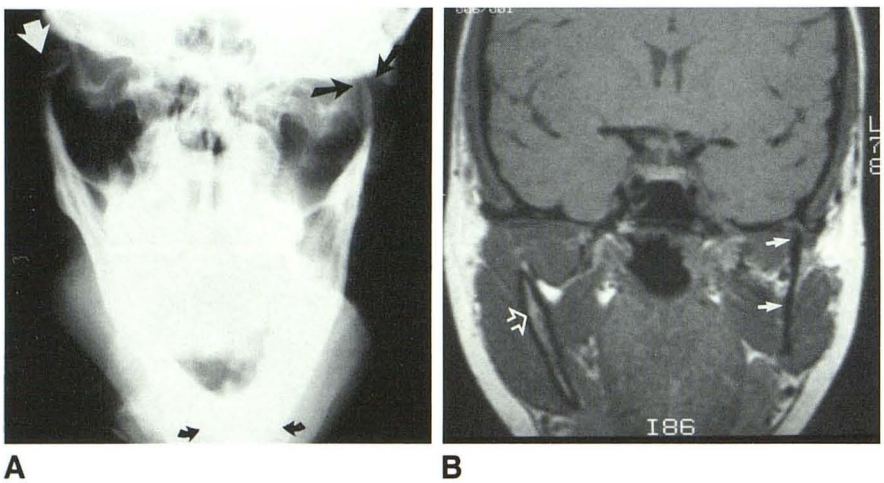

Fig. 11.—Skeletofacial deformity secondary to old avascular necrosis in 29-year-old woman with progressive facial deformity (clinically diagnosed as facial hemihypertrophy) and malocclusion since mandible injury at age 12.

A, Frontal radiograph shows deviation of chin (*curved arrows*) toward deformed left condyle (*straight black arrows*). Normal right condyle (*white arrow*).

B, Coronal 3-mm image, 900/20, in head coil shows absence of marrow signal from condyle and condylar neck (*solid arrows*) on left. Normal side (*open arrow*).

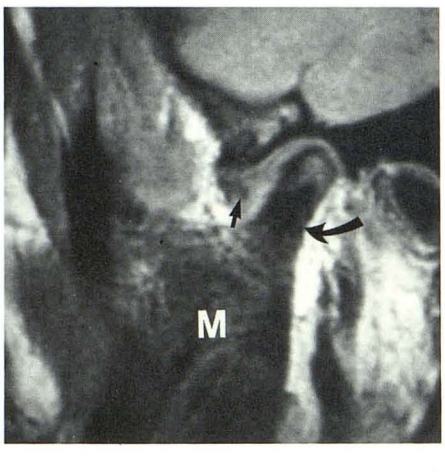

Fig. 12.—Complete loss of marrow signal within body of mandible (M) and condylar neck (*curved arrow*) associated with previous failed orthognathic surgery in 24-year-old woman with painless open bite (for 18 months) after failed surgery, performed to attempt correction of malocclusion. MR changes, bilateral. Sagittal image, 600/20, shows anteriorly displaced and severely deformed meniscus (*straight arrow*).

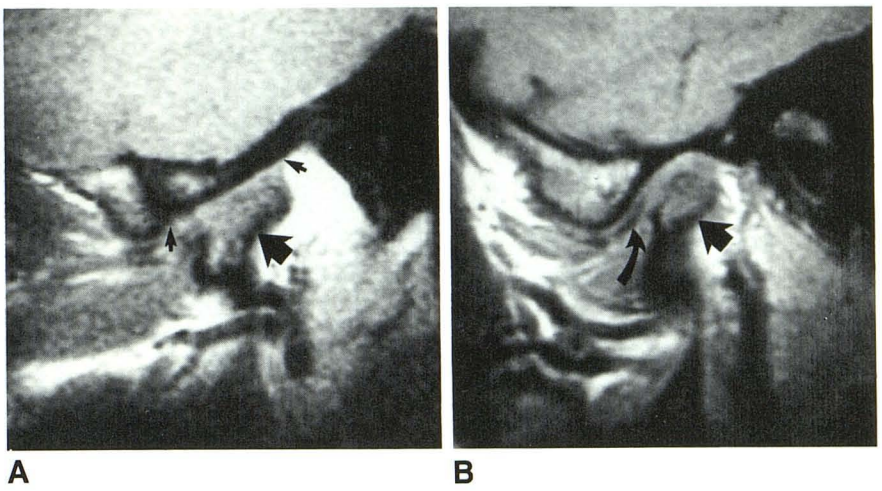

Fig. 13.—Old (*A*) and new (*B*) bilateral condylar avascular necrosis and meniscus derangements 3 months after failed orthognathic surgery in 15-year-old girl with painless openbite and retrognathia after unsuccessful initial orthodontics and subsequent sagittal split mandibular osteotomies, followed by 7½ weeks of intermaxillary fixation.

***A*, Sagittal image, 600/20, of left joint shows decreased signal from deformed condyle (*large arrow*). Note flattened articular surfaces of condyle and temporal bone (*small arrows*), suggesting long-standing disease. Tomograms revealed profound osseous sclerosis.**

***B*, Decreased condylar signal (*straight arrow*) in opposite joint with displaced meniscus (*curved arrow*).**

8–11, and 15) [14, 24–27]. We believe that many cases of acquired malocclusion, facial deformity, and condylar degeneration may be the consequence of AVN.

We found decreased marrow signal in cases of AVN on T1-weighted images (Table 3). Long TR/short TE images yielded variable signal characteristics with early AVN, healing, and OCD. Early AVN exhibited consistently high signal on T2-weighted images (Figs. 6, 7, 10, and 14) [14]. Acute OCD typically exhibited a hypointense central fragment surrounded by a zone of higher signal on both T1- and T2-weighted images (Figs. 2 and 3) [15]. We found GRASS images to be less reliable in evaluating these lesions than were either T1-weighted or long TR/short or long TE images due to the decreased spatial resolution and more variable signal characteristics associated with GRASS techniques [4, 21]. The MR findings associated with OCD and AVN in the mandibular condyle are similar to findings in the hips and major appendicular joints. The earliest detectable physiologic alteration in AVN appears to be vascular congestion with increased venous and capillary pressure, resulting in fluid transudation into the medullary space (Figs. 6, 7, 10, and 14) [14, 25]. MR is of particular value in detecting early lesions that may escape conventional radiographic detection. MR is also more accurate than scintigraphy in detecting early marrow changes prior to medullary infarction and structural collapse [9, 14, 16]. T2-weighted images are most helpful in demonstrating the early changes of marrow congestion and inflammation, both of which increase marrow fluid and result in increased signal. Simultaneous bone necrosis, inflammation, and healing may be observed on T2-weighted images (Figs. 6, 10, and 14). With late healing, there is replacement of normal, fat-containing hematopoietic marrow by hypointense fibrous tissue and sclerotic bone, resulting in loss of normal marrow signal (Figs. 8–12 and 14) [8, 12–14, 16]. Facial and joint pain; mechanical TMJ symptoms such as clicking, locking, and crepitus; and changing occlusion may be clinical hallmarks of ongoing necrosis, inflammation, and repair within the condyle and TMJ.

Radiologic changes of OCD and AVN are frequently observed in conjunction with joint effusion and internal derangement of the TMJ meniscus (Figs. 2, 3, and 5–16). This association suggests that meniscus derangement and joint inflammation may initiate marrow inflammation. A high prevalence of pathologic hip effusion has been associated with acute and subacute AVN of the femoral head [10]. We have observed areas of subarticular decreased MR signal within the condyle after perforation of the disk or meniscus attachments, particularly when there is associated erosion of the overlying articular-bearing-surface cartilage (Figs. 2, 6, 9, and 10). Postmortem studies have shown that subcortical cystic change, marrow fibrosis, and osseous sclerosis frequently are found in degenerated or remodeled condyles beneath areas of cartilaginous erosion [28, 29]. These observations suggest that internal derangement of the TMJ, which often progresses to perforation, precedes and may initiate the development of either OCD or localized AVN and subsequent structural osseous changes.

Previous investigations have shown that blood supply to the condyle and condylar neck (proximal mandibular segment) may be significantly reduced after sagittal split mandibular osteotomy, especially if the split is proximal and associated with muscle stripping along the medial periosteal surface of the condylar neck [2, 30, 31]. AVN of the proximal mandibular segment may occur as a complication of orthognathic surgery and lead to malocclusion and facial deformity (Figs. 12 and 13) [2, 3, 31]. We believe that the postoperative altered condylar stress loading and joint immobilization during intermaxillary fixation may either initiate or aggravate meniscus derangement and lead to AVN (Figs. 12 and 13). We have observed both acute medullary congestion and internal derangement with nonsurgical condylar repositioning and altered stress loading (Fig. 7). The diagnosis of AVN and/or internal derangement of the TMJ meniscus before either nonsurgical occlusal adjustment or orthognathic surgery is of vital importance for treatment planning. We believe that a significant number of failed occlusal adjustment procedures, including orthognathic surgery, may be secondary to preexisting internal derangement of the TMJ and/or AVN. Condylar AVN and internal derangement of the TMJ should be considered in all cases of orthognathic surgical failure.

Because mandibular condyle OCD and AVN generally are not recognized, there are no accepted therapeutic measures. We suggest prompt "unloading" of the condyle once a diag-

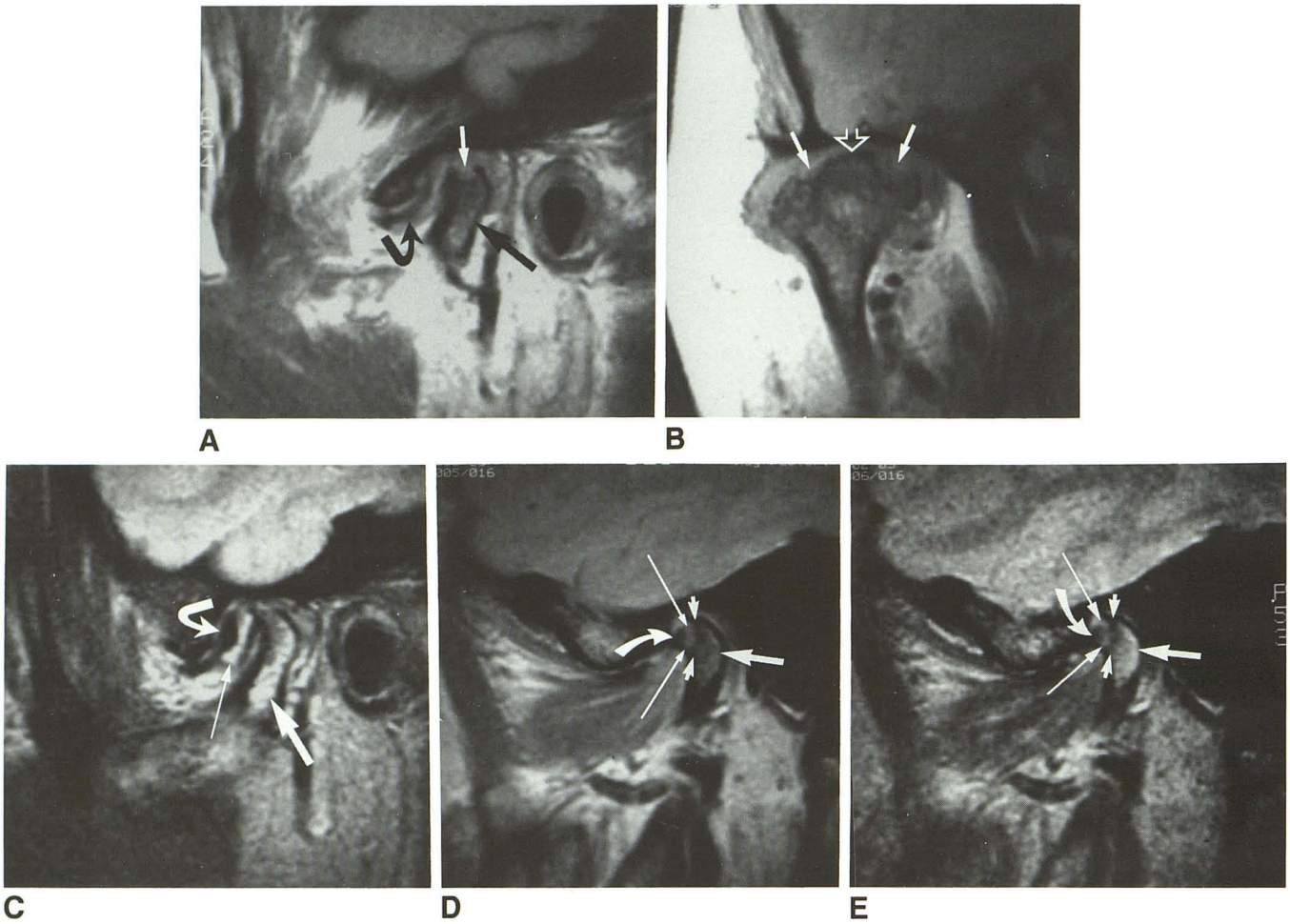

Fig. 14.—Acute and chronic avascular necrosis with changes of unstable osteochondritis dissecans in 46-year-old woman with clinically locked (frozen) joint and constant pain after jaw trauma 9 months before imaging.

***A*, Sagittal closed-mouth image, 600/20, through lateral pole of condyle reveals decreased marrow signal (*straight black arrow*) and sharply defined condylar defect (*white arrow*). Note meniscus (*curved arrow*) displacement and deformity.**

***B*, Coronal image, 600/20, reveals irregular and decreased marrow signal with medial and lateral corticomedullary defects (*solid arrows*) adjacent to area of intact cortex (*open arrow*).**

***C*, Sagittal image, 2200/80, reveals increased medullary signal (*large straight arrow*) with surgically proved organized hematoma (*smaller straight arrow*) beneath displaced meniscus (*curved arrow*).**

***D* and *E*, Sagittal images, 2200/20 (*D*) and 2200/80 (*E*), through medial pole of condyle reveal necrotic cortical bone (*curved arrows*); zone of healing and repair (*long straight arrows*); zone of sclerosis (*small straight arrows*); and inflamed, congested marrow (*large straight arrows*). At surgery, entire meniscus and subjacent hematoma were adherent to glenoid fossa and condyle, resulting in "frozen joint." Condyle exhibited alternating areas of both increased and decreased vascularity and foci of intact and eroded articular cartilage. Organizing clots were present within condylar depressions (*A* and *B*).**

nosis of active OCD or AVN is made. This can be accomplished by removal of any offending appliances or hardware to relieve condylar stress loading (articular weight-bearing). Any systemic illnesses should be treated appropriately, and iatrogenic factors such as exogenous steroids or chemotherapeutic agents should be modified if possible. Coexisting joint inflammation and meniscus derangement may require surgical intervention. Electrical bone-growth stimulation shows promise in promoting healing in the femoral head [7, 14]. Additional clinical experience with mandibular condyle lesions is needed.

We believe that the recognition of mandibular condyle OCD and AVN as existent disease entities will likely alter therapeutic approaches to patients with occlusal disorders and/or TMJ derangements. The relation between meniscus derangements, joint inflammation, and AVN merits further investigation. We advise the radiologic evaluation of patients with suspected AVN or internal derangement of the TMJ with radiography, tomography, and MR. MR should be used whenever a history of acquired or unstable malocclusion is elicited, and in all cases of either unexplained joint pain or clinically progressive internal derangement of the TMJ. We believe that many orthognathic surgical failures can be avoided if internal derangement of the TMJ meniscus and/or AVN are identified preoperatively. Meniscectomy may be required before orthognathic surgery in cases of malocclusion or facial deformity where meniscus derangement and inflammatory arthropathy

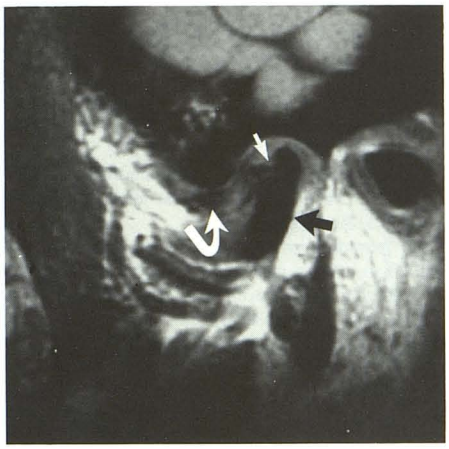

Fig. 15.—Extensive avascular necrosis, osseous deformity, condylar defect compatible with unstable osteochondritis dissecans, and advanced internal derangement of temporomandibular joint in 37-year-old woman with 10-month history of temporomandibular joint pain, locking, and acquired occlusal deficit. Sagittal MR image, 600/20, shows complete absence of marrow signal from both condyle and condylar neck (*black arrow*). Large articular surface defect (*straight white arrow*) is observed with late-stage meniscus (*curved arrow*) derangement. Surgery, 7 months after imaging, revealed depressed, pitted articular surface with partial resurfacing of condyle by fibrous tissue.

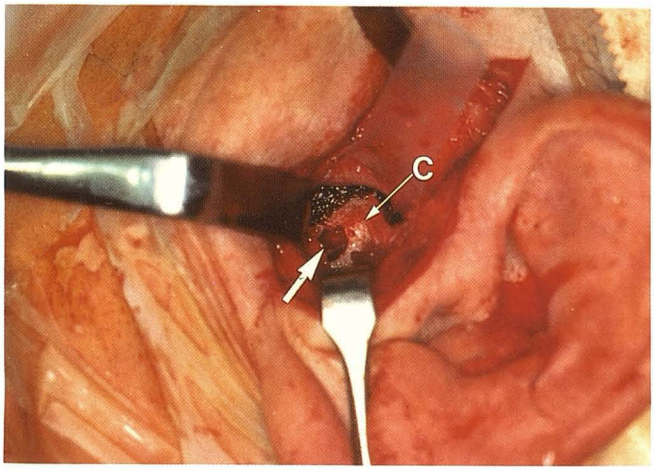

Fig. 16.—Unstable osteochondritis dissecans vs focal avascular necrosis in 52-year-old woman with long history of rheumatoid arthritis and several-month history of bilateral temporomandibular joint pain and locking (osseous condylar change unilateral). Intraoperative photography shows organizing clot (*arrow*) within condylar (C) defect. Necrotic condylar fragments (not shown) removed from joint surgically.

are demonstrated with MR. We advise caution in contemplating orthognathic surgical procedures in patients with active (especially inflammatory) TMJ arthropathy and/or narrow lesions of the mandibular condyle.

ACKNOWLEDGMENTS

We thank Kenneth B. Heithoff, Robert J. Keck, Robert B. Gillum, Steven D. Johnson, Albert Hohmann, Gary D. Lunstad, John J. Norton, Jeffrey A. Jahn, the technical staff at the Center for Diagnostic Imaging, and Becky Borgerson for contributions. Special credit to Allan B. Reiskin for his earlier work and conclusions.

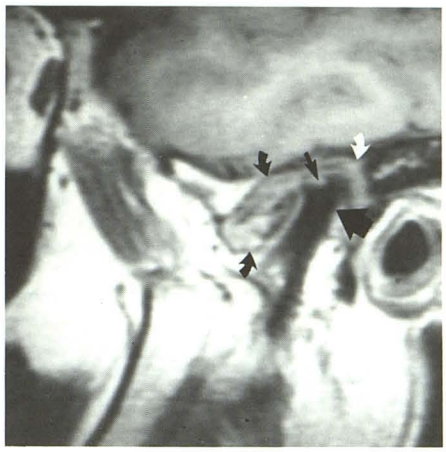

Fig. 17.—29-year-old woman with joint pain, dysfunction, crepitus, swelling, and worsening malocclusion 18 months after meniscectomy and permanent Proplast implant insertion. Destructive granuloma (*curved arrows*) fills joint capsule. Defect in articular surface of condyle (*small straight arrow*) secondary to direct granulomatous penetration through condylar surface. Absent marrow signal within condyle (*large straight arrow*) and condylar neck. (Reprinted from [3].)

REFERENCES

1. Reiskin AB. Aseptic necrosis of the mandibular condyle: a common problem? *Quintessence Int* **1979**;2:85–89
2. Behrman SJ. Complications of sagittal osteotomy of the mandibular ramus. *J Oral Surg* **1972**;30:554
3. Schellhas KP, Wilkes CH, Fritts HM, Omlie MR, Heithoff KB, Jahn JA. Temporomandibular joint: MR imaging of internal derangements and postoperative changes. *AJNR* **1987**;8:1093–1101, *AJR* **1988**;150(2):381–389
4. Schellhas KP, Wilkes CH, Omlie MR, et al. The diagnosis of temporomandibular joint disease: two-compartment arthrography and MR. *AJNR* **1988**;9:579–588, *AJR* **1988**;151:341–350
5. Schellhas KP, Wilkes, CH, El Deeb M, Lagrotteria LB, Omlie MR. Permanent Proplast temporomandibular joint implants: MR imaging of destructive complications. *AJR* **1988**;151:731–735
6. Totty WG, Murphy WA, Ganz WI, Kumar B, Daum WJ, Siegel MA. Magnetic resonance imaging of the normal and ischemic femoral head. *AJR* **1984**;143:1273–1280
7. Ficat RP. Idiopathic bone necrosis of the femoral head: early diagnosis and treatment. *J Bone Joint Surg [Br]* **1985**;67B:3–9
8. Thickman D, Axel L, Kressel HY, et al. Magnetic resonance imaging of avascular necrosis of the femoral head. *Skeletal Radiol* **1986**;15:133–140
9. Mitchell MD, Kundel HL, Steinberg ME, Kressel HY, Alavi A, Axel L. Avascular necrosis of the hip: comparison of MR, CT, and scintigraphy. *AJR* **1986**;147:67–71
10. Mitchell DG, Rao VM, Dalinka MK, et al. MRI of the joint fluid in the normal and ischemic hip. *AJR* **1986**;146:1215–1218
11. Mitchell DG, Rao VM, Dalinka MK, et al. The distribution of fatty and hemopoietic marrow in the normal and ischemic hip. *Radiology* **1986**;161:199–202
12. Gillespy T III, Genant HK, Helms CA. Magnetic resonance imaging of osteonecrosis. *Radiol Clin North Am* **1986**;24:193–208
13. Markisz JA, Knowles RJR, Altchek DW, Schneider R, Whalen JP, Cahill PT. Segmental patterns of avascular necrosis of the femoral heads: early detection with MR imaging. *Radiology* **1987**;162:717–720
14. Mitchell DG, Rao VM, Dalinka MK, et al. Femoral head avascular necrosis:

Correlation of MR imaging, radiographic staging, radionuclide imaging, and clinical findings. *Radiology* **1987**;162:709–715

15. Mesgarzadeh M, Sapega AA, Bonakdarpour A, et al. Osteochondritis dissecans: analysis of mechanical stability with radiology, scintigraphy, and MR imaging. *Radiology* **1987**;165:775–780
16. Beltran J, Herman LJ, Burk JM, et al. Femoral head avascular necrosis: MR imaging with clinical-pathologic and radionuclide correlation. *Radiology* **1988**;166:215–220
17. Shuman WP, Castagno AA, Baron RL, Richardson ML. MR imaging of avascular necrosis of the femoral head: value of small-field-of-view sagittal surface-coil images. *AJR* **1988**;150:1073–1078
18. Harms SE, Wilk RM, Wolford LM, et al. The temporomandibular joint: magnetic resonance imaging using surface coils. *Radiology* **1985**;157:133–136
19. Katzberg RW, Bessette RW, Tallents RH, et al. Normal and abnormal temporomandibular joint: MR imaging with surface coil. *Radiology* **1986**;158:183–189
20. Schellhas KP, Wilkes CH, Heithoff KB, Omlie MR, Block JC. Temporomandibular joint: diagnosis of internal derangements using magnetic resonance imaging. *Minn Med* **1986**;69:516–519
21. Schellhas KP, Fritts HM, Heithoff KB, Jahn JA, Wilkes CH, Omlie MR. Temporomandibular joint: MR fast scanning. *J Craniomandib Pract* **1988**;6:209–216
22. Schellhas KP, El Deeb M, Wilkes CH, et al. Three-dimensional computed tomography in maxillofacial surgical planning. *Arch Otolaryngol Head Neck Surg* **1988**;114:438–442
23. Chiroff RT, Cooke PC. Osteochondritis dissecans: a histologic and microradiographic analysis of surgically excised lesions. *J Trauma* **1975**;15:689–696
24. Glimcher MJ, Kenzora JE. The biology of osteonecrosis of the human femoral head and its clinical implications (three parts). *Clin Orthop* **1979**;138:284–309, 139:283–312, 140:273–312
25. Sweet DE, Madewell JE. Pathogenesis of osteonecrosis. In: Resnick DK, Niwayama G, eds. *Diagnosis of bone and joint disorders*. Philadelphia: Saunders, **1988**:3188–3237
26. Hughston JC, Hergenroeder PT, Courtney BG. Osteochondritis dissecans of femoral condyle. *J Bone Joint Surg [Am]* **1984**;66:1340–1348
27. Resnick D, Goergen TG, Niwayama G. Transchondral fractures (osteochondritis dissecans). In: Resnick D, Niwayama G, ed. *Diagnosis of bone and joint disorders*, vol. 5. Philadelphia: Saunders, **1988**:2795–2812
28. Debont LGM. *Temporomandibular joint articular cartilage structure and function* [doctoral thesis]. Groningen, the Netherlands: University of Groningen, **1985**
29. Debont LGM, Boering G, Liem RSB, et al. Osteoarthritis and internal derangement of the temporomandibular joint: a light microscopic study. *J Oral Maxillofac Surg* **1986**;44:634–643
30. Grammer FC, Meyer MW, Richter KJ. A radioisotope study of the vascular response to sagittal split osteotomy of the mandibular ramus. *J Oral Maxillofac Surg* **1974**;32:578–582
31. Kaplan PA, Tu HK, Koment MA, Ruskin JD, Bennion J. Radiography after orthognathic surgery. Part II: Surgical complications. *Radiology* **1988**;167:195–198